Experimental Trauma Surgery
Medical Faculty
Justus-Liebig University of Giessen (Germany)

2022 Proceedings of the 4th International Conference on Trauma Surgery Technology in Giessen

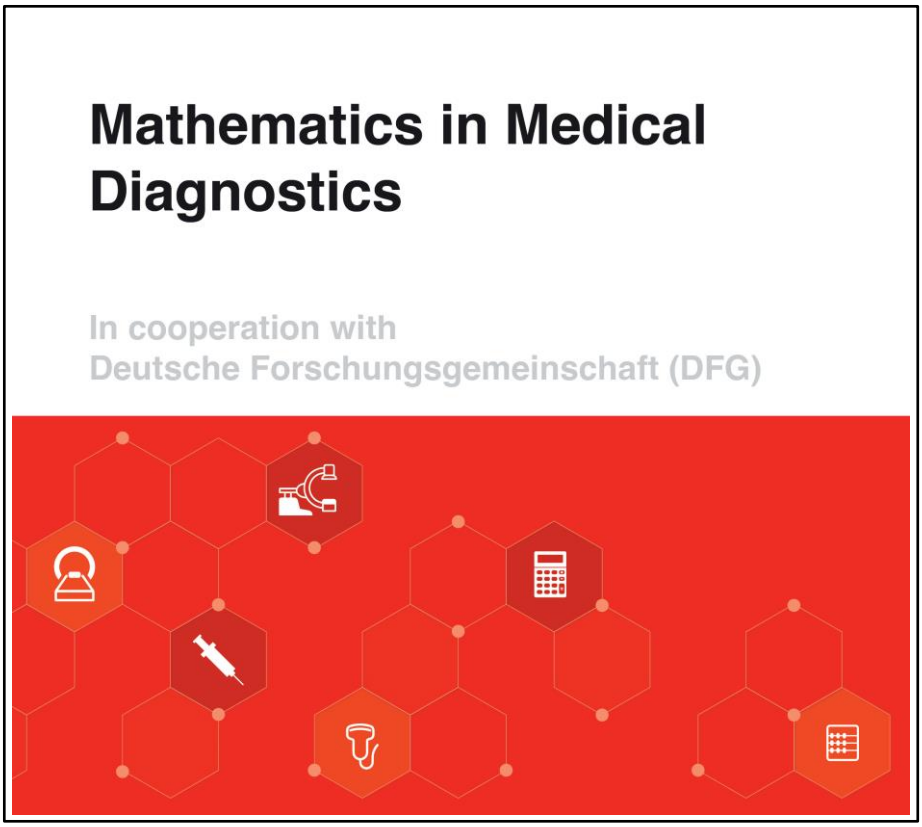

23 April 2022
In collaboration with
Deutsche Forschungsgemeinschaft

University Medical Faculty
Giessen (Germany)

2022 Proceedings of the 4th International Conference on Trauma Surgery Technology
Editors: WA Bosbach, JF Senge, P Dlotko

Conference Organisation and Editors of the Proceedings
WA Bosbach (Justus-Liebig University of Giessen, Germany)
JF Senge (University of Bremen, Germany)
P Dlotko (Justus-Liebig University of Giessen, Germany)

Approved funding by
Deutsche Forschungsgemeinschaft (DFG)
Grant recipients WA Bosbach (coordinator), P Dlotko
DFG grant BO 4961/11-1

4th (virtual/face-to-face hybrid) conference: Mathematics in medical diagnostics
DFG grant BO 4961/11-1
23 April 2022
Proceedings DOI *tbd*

3rd (virtual) conference: Multifunctional trauma surgery implants
DFG grant BO 4961/6-1
17 Oct 2020
Proceedings DOI 10.17863/CAM.60559
Closing talk “Osteosarcoma in a Dinosaur” DOI /10.17863/CAM.60210

2nd conference: Vibration in oncological and antibacterial therapy
DFG grant BO 4961/3-1
11 - 13 Oct 2019
Proceedings DOI /10.17863/CAM.45844

1st conference: Patient centred technology design in traumatology
DFG grant BO 4961/4-1
16 - 18 Nov 2018
Proceedings DOI /10.17863/CAM.34582

Correspondence

Wolfram A. Bosbach, MD PhD
Research Associate and Radiology Resident
Department of Diagnostic, Interventional and Paediatric Radiology, Inselspital
University of Bern
10, Freiburgstrasse
Bern 3010
Switzerland
Email WolframAndreas.Bosbach@Insel.CH

Preface

Dear Colleagues

Dear Speakers

Dear guests who logged in at zoom on 23 April

The **4th** event of the **Giessen International Conference Series on Trauma Surgery Technology** has taken place on **April, the 23rd 2022**. It was a great pleasure for us to host the event face to face from Warsaw (Poland) at the Max-Planck Dioscuri Centre for Topological Data Analysis (TDA, dioscuri-tda.org) while having in parallel virtual parts on zoom.

The same month, we had been able to publish a collaboration manuscript between the Polish team in Warsaw and the group of Prof Sara Bagherifard from POLIMI (Milano, Italy) who spoke in Giessen at the 2018 event. The research investigates by the application of TDA how conventional surface roughness measures can be extended to better capture surface morphology. The surface input geometries came from Milan. The TDA pipeline constructed built persistence diagrams and Betti curves:

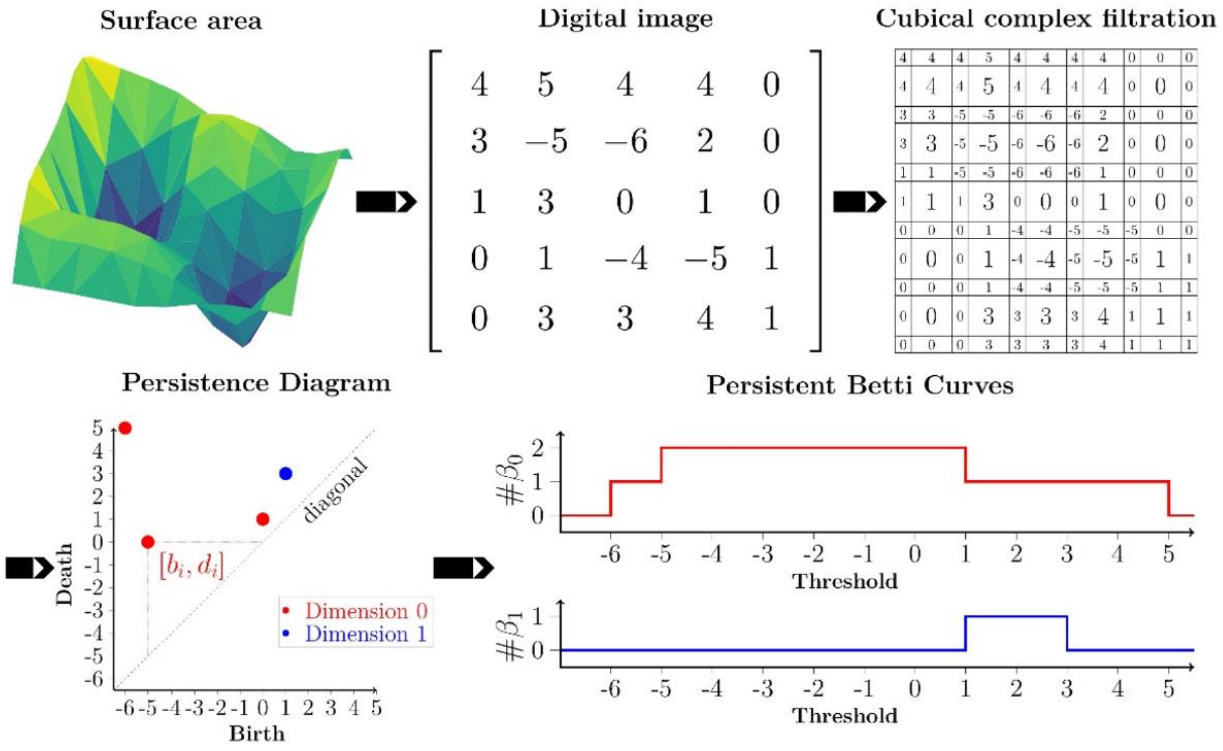

Figure: Pipeline for the calculation of persistent diagrams and Betti curves (BC) in dimension 0 and 1: the surface is interpolated on a regular grid to obtain a digital image; the pixels of which are converted to top-dimensional cells of a 2-dimensional cubical complex. We obtain the birth and death values of points in the persistent diagram in dimension 0 and 1. Counting the number of connected components and holes for different thresholds in the filtration gives us the BC [1].

Input files, code, and further documents are accessible on github: github.com/janfsenge/tda_shotpeening.git. The research is aimed at better capturing surface

morphologies and at improving surface applications in the medical field (ie biocompatibility or corrosion resistance) or outside in non-medical applications (wear, fatigue, friction etc).
The manuscript, available now [1], is only one of many examples where **advanced mathematics**, such as TDA, can improve engineering solutions and make innovation accessible.

The 2022 event was specifically held to bring together practical application research, with a focus on medical imaging, and the TDA experts from Warsaw.
Our hope is that the talks and conversations have created stimulus for further research projects. We have already started the preparations for the next event in 2023/24.

Your scientific committee

Reference:
[1] J. F. Senge, A. Heydari Astaraee, P. Dlotko, S. Bagherifard, and W. A. Bosbach, “Extending conventional surface roughness ISO parameters using topological data analysis for shot peened surfaces,” Sci. Rep., vol. 12, no. 5538, pp. 1–12, 2022.

Programme with presented abstracts

Opening session

Starting 1 pm

- **Dlotko, Pawel, Dioscuri Centre for Topological Data Analysis, Warszawa, Poland**
  Welcome message, technical details and workshop structure
  How to see multiple clinical parameters acting together?

Session 1 – Topological data analysis, Chair: Bosbach, Wolfram A

Starting 1.30 pm

- **Senge, Jan, Department of Mathematics and Computer Science, University of Bremen, Germany**
  Analysis of synchrotron images of human femoral heads and extraction of their topological characteristics
- **Hellmer, Niklas, Dioscuri Centre for Topological Data Analysis, Warszawa, Poland**
  Metrics for persistence diagrams and modules and interactions of TDA with statistics
- **Gurnari, Davide, Dioscuri Centre for Topological Data Analysis, Warszawa, Poland**
  Distributed computations of persistence curves and extensions of mapper-type algorithms

Coffee break 15 min

Session 2 – Non-TDA works, Chair: Dlotko, Pawel

Starting 2.45 pm

- **Tindall, Marcus J, Department of Mathematics and Statistics & Institute of Cardiovascular and Metabolic Research, University of Reading, UK**
  Mathematical modelling of bacterial chemotactic systems – The Rhodobacter sphaeroides case example
- **Burfitt, Matthew, Department of Mathematics, University Aberdeen, UK**
  A projective model for fast field cycling MRI images
- **Bosbach, Konstantin E, Medical Department, University of Freiburg, Germany**
  Investigating in vivo Detectability of the Neurotransmitter GABA in Magnetic Resonance Spectroscopy with the Monte Carlo method

Coffee break 15 min

Session 3 – Medical applications, Chair: Senge, Jan F

Starting 4.00 pm

- **Bosbach, Wolfram A, Department of Diagnostic, Interventional and Paediatric Radiology (DIPR), Inselspital, Bern University Hospital, University of Bern, Switzerland**
  VBA simulations of hospital operations – case study on Covid-19 vaccine rollout schemes
- **Ramedani, Saied, Graduate School of Cellular and Biomedical Sciences, University of Bern, Switzerland**
  Automated Evaluation of the Whole Body's Muscle-fat Composition by Machine Learning for Magnetic Resonance Images (MRI)
- **Maryanski, Marek, Institute of Nanotechnology and Material Science, Gdansk University of Technology, Poland**
  Towards automatic comparison between planned stereotactic radiosurgery dose distributions and those measured from high-definition 3D gel dosimetry images
- **Haupt, Fabian, Department of Diagnostic, Interventional and Paediatric Radiology (DIPR), Inselspital, Bern University Hospital, University of Bern, Switzerland**
  Educational presentation of state of the art imaging of congenital vascular malformations

2022 Proceedings of the 4th International Conference on Trauma Surgery Technology
Editors: WA Bosbach, JF Senge, P Dlotko

Opening session

How to see multiple clinical parameters acting together?

Dlotko Pawel*, Gurnari Davide

Centre in Topological Data Analysis, Mathematical Institute of the Polish Academy of Sciences, Warsaw, Poland

* corresponding author, pdlotko@impan.pl

Introduction Plots of various types are fundamental tools in data analysis. Take a result of standard blood tests; for any given patient they measure a number of 15-20 parameters from a blood sample. The reference ranges of those parameters are obtained when analogous measurements are made for sufficiently large healthy population. Typically they are constructed in the way that 95% of the healthy population have the considered parameter in this range. The 2.5% of healthy population as well as population suffering from some disease will be scoring below and above the reference range. The position of a score of a given patient is an indication of its health state. However, to get an accurate diagnosis, values of a number of parameters have to be taken into account simultaneously. Looking at the right parameters that are indication of health state or a certain diseased is the know-how of medical professionals.

In this extended abstract we will show a methodology of Ball Mapper that may help visualizing the layout multiple parameters at the same time. In addition to the layout, the information if the given state correspond to healthy population, or a population suffering from some diseases can be added.

Ball Mapper In this section the basic idea of the Ball Mapper will be given. Take a point cloud X with a distance function $d: X \times X \to \mathbb{R}^{\leq}$ and a positive constant ε. An additional parameter may be an objective function $f: X \to \mathbb{R}$. In the case considered in our leading example [6], the point cloud consists of breast cancer gene expressions data discussed in [1]. As distance functions, Euclidean distance as well as cosine distance are considered. An objective function is either a binary variable indicating if a patient survived, or the variable indicating the expression level of the estrogen receptor gene.

An ε-net is a subset $Y \subset X$ such that for every $x \in X$ there exist $y \in Y$ such that $d(x,y) \leq \epsilon$. In this case we have that $X \subset \bigcup_{y \in Y} B(y, \epsilon)$. The Ball Mapper graph is an abstract graph constructed in the following way; points from Y correspond to vertices of the graph. In the visualization, the size of the vertex corresponding to a point $y \in Y$ will be proportional to the cardinality of $B(y, \epsilon) \cap X$. An edge is placed between two vertices corresponding to points $y_1, y_2 \in Y$ if and only if there exist $x \in X$ such that both $d(x, y_1) \leq \varepsilon$ and $d(x, y_2) \leq \varepsilon$.

A Ball Mapper graph of the set X with an objective function $f: X \to \mathbb{R}$ may be equipped with an induced function on its vertices. The value of a vertex corresponding to $y \in Y$ will be an average value of the function f for points in $B(y, \varepsilon) \cap X$. An idea of the construction is given at the Figure 1.

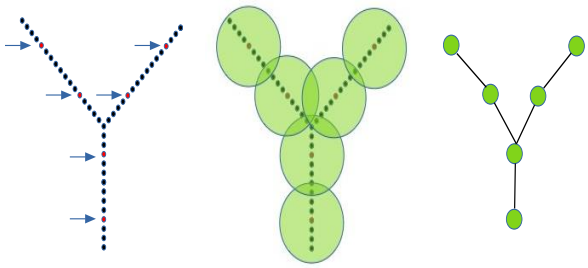

Figure 1. An idea of the construction of the Ball Mapper graph. Left; the point cloud X. Elements of the ε-net Y are indicated by arrows. Middle; the cover of X by ε radius balls centered in Y. Right; the Ball Mapper graph. Its vertices correspond to points in Y, edges, to nonempty intersections of balls centered in points from Y.

Analysis There are multiple analogous studies in which conventional mapper [3] was used for that purpose [4]. Also, some studies in this direction have been made using Ball Mapper in the context of Covid19 [5]. In this extended abstract we will showcase the whole pipeline in which we will work on the NKI dataset [1]. The dataset consists of the genomic data of 272 patients. Each patient's record is composed of 1570 entries, hence it gives 272 points in 1570–dimensional space. The first 17 columns consist of patient's info (some of them being self-explanatory) named ID, AGE, EVENTDEATH, SURVIVAL, TIMERECURRENCE, CHEMO, HORMONAL, AMPUTATION, HISTTYPE, DIAM, POSNODES, GRADE, ANGIOINV, LYMPHINFIL, BARCODE, ESR1. The remaining are genomic expression, and they are used as a feature in this studies. The colouring variable that we want to plot on the top of genomic expression is the variable EVENTDEATH that occurred for 28% of considered patients. The code presenting the whole analysis is available at a jupyter notebook available at [6].

In our first approach, we are using the Euclidean distance between the points to construct Ball Mapper graph. As we can see from the accompanying jupyter notebook and the Figure 2, this study does not reveal much. The reason for that is so called *concentration of measure phenomena*. It typically happens for unstructured data in high dimensions and manifest itself in a phenomenon that a distance between any pair of points is the same, regardless of the points. Clearly, in this extra case, trying to cover the dataset with collection of balls is meaningless, as either, for low values of ε we will see individual points solely covered by the balls centered in them, of we will see one ball covering all the points. In both cases, the Ball Mapper graph has no meaning.

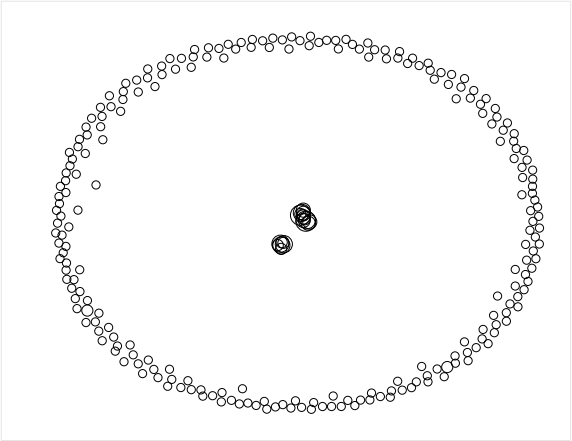

Figure 2. Ball mapper graph of the NKI dataset constructed based on Euclidean distance with $\varepsilon = 10$ colored by the binary variable indicating if the patient has

survived (white) or not (red). No visible structure can be found in the Ball Mapper graph.

As using Euclidean distance turned out not to be feasible, we can turn to use a so-called cosine similarity measure [2]. Given two vectors in $x, y \in \mathbb{R}^n$, it computes the cosine of an angle between them. This may be easily achieved by computing the dot product of the normalized vectors. When this distance is user, as we can observe at the Figure 3, much better separation of the class of patients that survive and the one that does not, is obtained. In particular,

In fact, by colouring the obtained cluster by other variables, we can determine that the survival is strongly correlated with the estrogen variable as it can be seen at the Figure 3.

Conclusions. This short note shows an example use of a Ball Mapper on a multidimensional dataset. It shows how a binary function of survival, influenced by 1570 variables, can be effectively visualized.

This exploratory data analysis technique shows that it is possible to predict, based on the levels of multiple variables, prognosis for a given patient. In the considered case, the prognosis is strongly correlated with the cancer estrogen receptor status, however in a general case, it can simply be function of many variables. Ball Mapper allows to observe them acting together and hence may be used as exploratory tool in medical diagnostic.

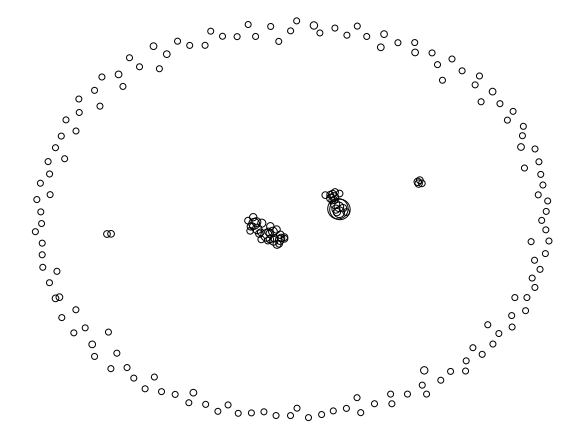

Figure 3. Ball mapper graph of the NKI dataset constructed based on cosine similarity with $\varepsilon = 0.43$ colored by the binary variable indicating if the patient has survived (white) or not (red). Over here a clear separation of the patients that survived from those that not is visible.

Bibliography

[1] P. Y. Lum, G. Singh, A. Lehman, T. Ishkanov, M. Vejdemo-Johansson, M. Alagappan, J. Carlsson & G. Carlsson, Extracting insights from the shape of complex data using topology, Scientific Reports volume 3, 1236 (2013).

[2] Amit Singhal, Modern Information Retrieval: A Brief Overview, Bulletin of the IEEE Computer Society Technical Committee on Data Engineering 24 (4): 35–43, 2001.

[3] Gurjeet Singh, Facundo Memoli, Gunnar Carlsson, Topological Methods for the Analysis of High Dimensional Data Sets and 3D Object Recognition, Eurographics Symposium on Point-Based Graphics, 2007.

[4] Monica Nicolau, Arnold J. Levine, Gunnar Carlsson, Topology based data analysis identifies a subgroup of breast cancers with a unique mutational profile and excellent survival, PNAS 2011.

[5] Pawel Dlotko, Simon Rudkin, Covid-19 clinical data analysis using Ball Mapper, doi.org/10.1101/2020.04.10.20061374
[6] D. Gurnari, Example 5, NKI dataset, github.com/dgurnari/pyBallMapper/tree/main/notebooks, data accessed for 15 May 2022

Conflict of interest

The authors declare that there are no conflicts of interest.

Acknowledgment

PD and DG acknowledge support by Dioscuri program initiated by the Max Planck Society, jointly managed with the National Science Centre (Poland), and mutually funded by the Polish Ministry of Science and Higher Education and the German Federal Ministry of Education and Research.

2022 Proceedings of the 4th International Conference on Trauma Surgery Technology
Editors: WA Bosbach, JF Senge, P Dlotko

Session 1 – Topological data analysis

Analysis of synchrotron images of human femoral heads and extraction of their topological characteristics

J.F. Senge[1], P. Dłotko[2], D. Gurnari[2], L. M. Vergani[3], and F. Buccino[3]

[1]Institute for Algebra, Geometry, Topology and their Application, Department 3: Mathematics / Computer Science, University of Bremen, Bremen, Germany

[2]Dioscuri Centre in Topological Data Analysis, Mathematical Institute of the Polish Academy of Sciences, Warsaw, Poland

[3]Department of Mechanical Engineering, Politecnico di Milano, Milan, Italy

** corresponding author, janfsenge@uni-bremen.de*

Synchrotron images of human bones, while allowing to detect micro-scale damage phenomena, produce an impressive amount of high-resolution data with a strong impact on post-processing computational costs. In this context, we consider different approaches to assist the detection of bone micro-scale features, such as cracks and lacunae. This allows to shed some light on the interaction between multi-scale porosities and fractures in a 3D manner. More explicitly, starting from synchrotron images at a resolution of 1.6 μm of human femoral bones at progressively increasing compression levels, we detect bone cracks using a combination of various unsupervised approaches instead of a supervised learning approach using neural networks exploited in previous works. Furthermore, we consider some techniques of Topological Data Analysis – mainly the Euler characteristic curve, as a possible invariant for comparison between osteoporotic and healthy bone samples in conjunction with the existing BV/TV. This is a preliminary work and needs to be continued and expanded by a more thorough analysis of the different methods involved and their potential errors. Therefore, we will focus on various applications of Euler characteristic curves for understanding examples of the bone structure.

Background & Methods In recent years, there has been an increase in fragility fractures necessitating a better understanding on the causes and structures involved in the occurrence and anticipation of fracture propagation in human bones. These problems are now considered from a multi-scale perspective assigning importance to micro-scale phenomena as the key for the detection of early damage developments and as an aid to assess the bone quality in general [1]. Following the data presented in [2], we are considering several different synchrotron images for different stages of micro-compression, see Figure 1, and apply topological descriptors for the bone structure as well as understanding the lacunar network and crack formations during increasing time intervals.

The provided synchrotron images entail several different trabecular bone samples; in particular two healthy and two osteoporotic ones are presented. Each sample, with a square (4X4 mm) cross-section and a 6mm length, is subjected to four different micro-compression stages that lead to crack formation and propagation, and to synchrotron radiation after each micro-compression stage. For a detailed discussion of the data and the convolutional neural network approach, see [2], [3]. One large caveat of this approach is that due to computational costs, the training and test sets are only 2d image slices and the 3d nature of the synchrotron image can't be exploited.

Topological Data Analysis (TDA) is a field in mathematics interested in quantifying and exploring more about the shape of structures. It provides tools for multi-scale analysis of the geometric and topological properties of an object and has proved helpful in a plethora of different applications [4]. Persistent homology [5] is one of the most prominent techniques of TDA. It is based on the idea that for a suitable real-valued function $f: X \to \mathbb{R}$ describing the height of the surface X we can track the evolution of connected components and holes of f. This evolution is given by the homology groups of dimensions 0 and 1 of the sublevel sets $f^{-1}((-\infty, a]) = \{x \in X | f(x) \leq a\}$. In other words, the sublevel sets of f give a nested sequence of subspaces, $\emptyset = X_0 \subset X_1 \subset \ldots \subset X_n = X$, called filtration. For the computations, we need suitable combinatorial structures for these subspaces, for images these are cubical complexes. Hence, we have a filtration of cubical complexes $K_0 \subset K_1 \subset \cdots \subset K_n$. Keeping track of homology of these subspaces / subcomplexes gives the persistence diagram of the surface X with the height function f.

While progress has been made in terms of efficiency, one drawback of persistent homology is that computing it for very large datasets is still computationally too expensive. One solution is to take an invariant which is easier to compute and can be calculated in a streaming fashion even though some information is lost. One such invariant is the Euler characteristic curve (ECC). The ECC is based on the topological invariant of the Euler-Poincare characteristic – also called Euler number. This is often given in the form for a discrete 2-dimensional surfaces M, like triangulations of a torus, as the alternative sum of the number of vertices V, edges E and faces F of M:

$$\chi(M) = \#V(M) - \#E(M) + \#F(M).$$

Another, equivalent definition is given by the alternative sum of the number of connected components, the number of tunnels and the number of voids of M. These are the 0-th, 1-th and 2-nd Betti numbers of M:

$$\chi(M) = \beta_0(M) - \beta_1(M) + \beta_2(M).$$

This is exactly what gives this characteristic its usefulness: We can capture global topological information in the form of holes using local computations by summing up vertices, edges, and faces, see [6] The Euler Characteristic Curve is a function which assigns the Euler number $\chi(K_i)$ to each of the complexes K_i of the filtration. In the case of grayscale images, the function used to get a filtration is the

function assigning each voxel for 3d-images or pixel for 2d-images one grayscale value in $\{0, 1, \dots, 255\}$.

Results As already shown in [1], the propagation of cracks in the bone is influenced by the lacunar network for the different cracks in the bone. While our methods for the detection of bone cracks and lacunae can be used in a 3d setting, the neural network approach also bears merits in being able to provide a better detection rate for different types of cracks. Hence, the neural network approach generalizes well in terms of bone crack detection depending on the selection of training samples provided.

The findings for lacunae and bone cracks found by our methods are therefore similar to the ones found by the neural network approach, while giving a better run-time due to the omission of training of the neural network. A deeper comparison between the findings of the different methods is underway.

In contrast to the local algorithms, focusing on certain sub-volumes in the bone and their Euler characteristic curves gives a clustering into healthy patients and osteoporotic samples.

Using the whole image stack for each patient and the associated Euler characteristic was not done, due to slow run-time and limitations on the number of samples. Hence, subsamples where taken. For them to be comparable, we also considered the bone volume over the total volume, BV/TV, values in the clustering considerations.

In Figure 2 we show 6 lines corresponding to the BV/TV of image stacks of size 100x3678x3678 of the synchrotron images from healthy and osteoporotic patients in different compression steps. We can see that the values are relatively similar except the outliers for the last compression step. The reasons for this are that many smaller bone fragments in this step make the distinction between artifacts and bone sample difficult.

To showcase how the Euler characteristic curves (ECCs) are more sensitive to differences between the healthy and osteoporotic bone samples, we plot the ECCs in Figure 3, as rows in a heatmap where the pixel values, for the grayscale value t, correspond to the Euler number $\chi(K_t)$ of the cubical complex K_t in the filtration of the image stack of health/osteoporotic patients in different compression steps. Visually, we see a difference between healthy and osteoporotic patients. For a proper statistically sound analysis of a classifier for this binary problem, more data samples are needed than the ones shown here. Thus, the results of the classifier supporting the findings in Figure 3 are not shown here.

Conclusion The large synchrotron images for different stages of micro-compression provide good opportunities for a detailed analysis with the aim of understanding interdependencies of structures in a micro-scale perspective. One burden for this analysis is to find suitable algorithms and descriptors of the different objects of interest which are suitable for the large amount of information to be analyzed. While the neural network approach in [1] shows very good results, the computational time needed prevents practical use for the

complete image stack. TDA can help in understanding the topological information encoded in the bone structure and there exists suitable descriptors which can be used for large datasets like the Euler Characteristic Curve. It should be noted that this is preliminary work and needs a proper statistical analysis to showcase how well ECCs can be used to distinguish differences between the different bone samples.

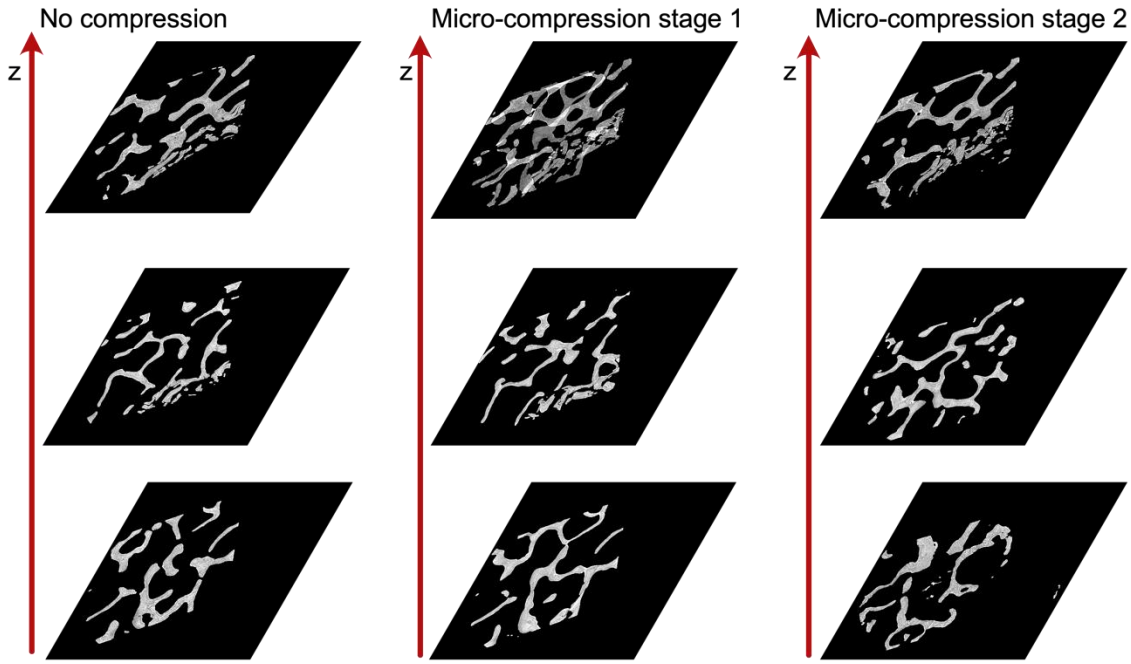

Figure 1: Synchrotron image slices for different z-positions and different compression stages. Images are of size 6141x3678x3678.

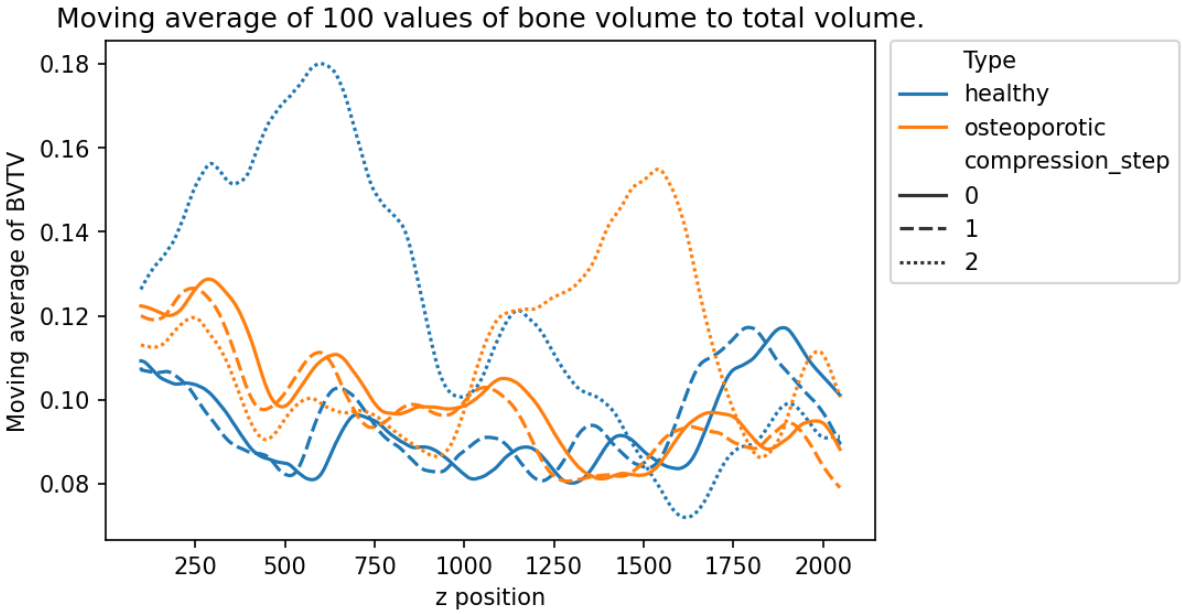

Figure 2: Moving average of 100 BVTV values of consecutive image slices (in z-direction) for healthy and osteoporotic patients for 2048 image slices.

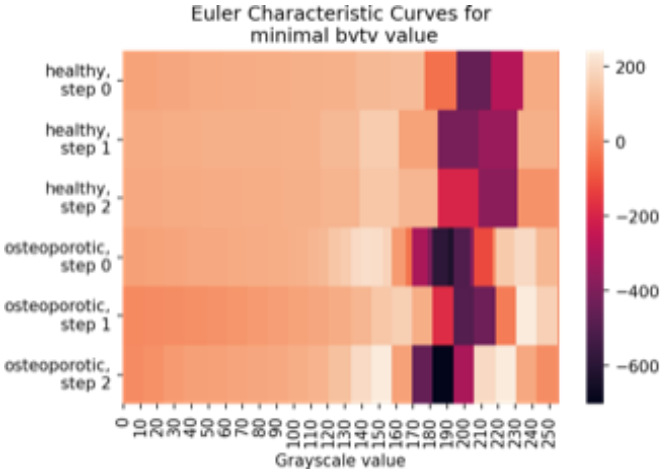

Type	100-Moving average BVTV
healthy, step 0	0.088
healthy, step 1	0.089
healthy, step 2	0.082
osteoporotic, step 0	0.088
osteoporotic, step 1	0.091
osteoporotic, step 2	0.103

Figure 3: Different ECCs for image stacks of size 100x3678x3678 corresponding to the minimal BVTV values shown in Figure 2. The ECC are shown as rows in the heatmap on the left. Each pixel corresponds to the Euler number for the cubical complex for which voxels are present if their value is smaller or equal to the grayscale value listed below.

Bibliography

[1] S. Ma et al., “Synchrotron Imaging Assessment of Bone Quality,” Clinical Reviews in Bone and Mineral Metabolism, vol. 14, no. 3, p. 150, Sep. 2016, doi: 10.1007/S12018-016-9223-3.

[2] F. Buccino et al., “Assessing the intimate mechanobiological link between human bone micro-scale trabecular architecture and micro-damages,” Engineering Fracture Mechanics, vol. 270, p. 108582, Jul. 2022, doi: 10.1016/J.ENGFRACMECH.2022.108582.

[3] F. Buccino et al., “Mapping local mechanical properties of human healthy and osteoporotic femoral heads,” Materialia (Oxf), vol. 20, 2021, doi: 10.1016/j.mtla.2021.101229.

[4] B. Zielinski, M. Lipinski, M. Juda, M. Zeppelzauer, and P. Dlotko, “Persistence codebooks for topological data analysis,” Artificial Intelligence Review, 2020, doi: 10.1007/s10462-020-09897-4.

[5] H. Edelsbrunner and D. Morozov, “Persistent Homology: Theory and Practice,” in European Congress of Mathematics, 2012, pp. 31–50.

[6] T. Heiss and H. Wagner, “Streaming Algorithm for Euler Characteristic Curves of Multidimensional Images,” Lecture Notes in Computer Science (including subseries Lecture Notes in Artificial Intelligence and Lecture Notes in Bioinformatics), vol. 10424 LNCS, pp. 397–409, May 2017, doi: 10.1007/978-3-319-64689-3_32.

Conflict of interest

The authors declare that there are no conflicts of interest.

Funding sources

JFS and PD acknowledge support by Dioscuri program initiated by the Max Planck Society, jointly managed with the National Science Centre (Poland), and mutually funded by the Polish Ministry of Science and Higher Education and the German Federal Ministry of Education and Research.

Session 2 – Non-TDA works

Mathematical modelling of bacterial chemotactic systems – The Rhodobacter sphaeroides case example

Marcus J Tindall[1,2] *

[1] *Department of Mathematics and Statistics, University of Reading, Whiteknights, Reading, United Kingdom, RG6 6AX.*

[2] *Institute of Cardiovascular and Metabolic Research, University of Reading, Whiteknights, Reading, United Kingdom, RG6 6AA.*

* corresponding author m.tindall@reading.ac.uk

Mathematical modelling of bacterial chemotactic systems serves as a paradigm for the application of mathematical modelling in the life sciences. Over a period of 50 years experimentalists and theoretical modellers have worked hand-in hand to understanding how the intracellular signalling cascade of bacterial species, specifically *Escherichia coli*, link to the overall physiological response of the cell. In this talk I will demonstrate how our development of mathematical models of the waterborne bacterial chemotactic species *Rhodobacter sphaeroides*, has helped in elucidating the signalling cascade behaviour within the cell and allowed us to postulate the role of specific intracellular signalling proteins in driving the overall cellular response. This work naturally accounts for the spatiotemporal variation of the protein concentration within the cell, given the spatial localisation of some proteins. I will demonstrate how our most recent work in this area raises new possibilities regarding the design structure of the cell in respect of the cell response and metabolism.

Bibliography

[1] Edgington, MP, de Beyer JA, Armitage JP and Tindall MJ. The cytoplasmic chemoreceptor cluster of Rhodobacter sphaeroides could detect the cell's intracellular metabolic state. In preparation.

[2] Kojadinovic M, Armitage JP, Tindall MJ and Wadhams G. Rhodobacter sphaeroides response kinetics: Complexities in signalling but similarities in responses. J. Royal. Soc. Interface, 10(81):20121001, 2013.

[3] Tindall MJ, Porter SL, Maini, PK and Armitage JP. Modeling chemotaxis reveals the role of reversed phosphotransfer and a bi-functional phosphatase, PLoS Comput. Biol., 6(8), e1000896, 2010.

Ethics approval

Research does not require ethics approval.

Conflict of interest

None

Funding sources

Biotechnology and Biological Sciences Research Council (BBSRC) and Engineering and Physical Sciences Research Council (EPSRC), UK.

2022 Proceedings of the 4th International Conference on Trauma Surgery Technology
Editors: WA Bosbach, JF Senge, P Dlotko

A projective model for fast field cycling MRI images

Burfitt, Matthew

Department of mathematics, University Aberdeen, Aberdeen, UK

* corresponding author, matthew.burfitt@abdn.ac.uk

Fast Field-Cycling MRI (FFC MRI) has the potential to recover new biomarkers form a range of diseases by scanning a number of lower magnetic field strengths simultaneously [1]. The images produced by an FFC scanner can be interpreted in the form of a sequence of times series of 2-dimensional grey scale images, with each time series corresponding to each of the different magnetic field strengths. In ongoing work, we investigate applications of data analysis and machine learning to brain images of ischemic and hemorrhagic stroke obtained using the FFC MRI scanner as part of the Puffins 2 study.

To analyses such images as a data point cloud, we extract features as vectors of image pixels values corresponding to the same spatial voxel location at each time and magnetic field strength. At present the FFC images have lower resolution than that those obtained from a 3T scanner, however they are equipped with the advantage of higher dimension obtained using the range of times and magnetic fields strengths. One obstacle to the analysis of MRI images also present for FFC MRI images are intensity inhomogeneity usually modeled as the multiplication of an image by some smoothly varying error surface. May algorithms have been developed with the aim of removing such errors [2]. However, a potently simple solution to this problem is to consider the time directional image features only up to multiplication by a constant. This we might interpreted as constructing an embedding of our point cloud into a product standard n-simplices.

The feature point cloud obtained through a joint projective embedding of features transforms the data at the expense of discarding some information. By direct observation and subsequent analysis of the reconstructed images form the transformed point cloud, we observe that the projective point cloud appears to provide a good model for tissue type while removing the structure of the tissue state in the region of the stroke legion.

To recover a segmentation of anomalous regions of the FFC images corresponding to stroke damaged tissue we must devise a procedure to identify the differences between the projective point cloud and the original feature point cloud. One way to obtain a simple model of the tissue types form our projective point could is to take its projection onto the first principal component, providing use with a single value assigned to each feature. We then consider the residual errors of a linear model, fitting tissue types against an image complementary to the projective embedding for each magnet field strength. The residuals assigned to each FFC MRI voxel now provide

a new image highlighting anomalous regions of the image indicating stroke damaged tissue.

Bibliography

1] Broche, L.M., Ross, P.J., Davies, G.R. et al. A whole-body Fast Field-Cycling scanner for clinical molecular imaging studies. Sci Rep 9, 10402 (2019)

[2] U. Vovk, F. Pernus and B. Likar, "A Review of Methods for Correction of Intensity Inhomogeneity in MRI," in IEEE Transactions on Medical Imaging, vol. 26, no. 3, pp. 405-421, March 2007

Ethics approval

North of Scotland Research Ethics Committee, IRAS Project ID: 279919.

Conflict of interest

The authors declare that there are no conflicts of interest.

Funding disclosure

Funded by Chief scientist's Office project grant, grant reference number: TCS/19/44.

2022 Proceedings of the 4th International Conference on Trauma Surgery Technology
Editors: WA Bosbach, JF Senge, P Dlotko

Investigating in vivo Detectability of the Neurotransmitter GABA in Magnetic Resonance Spectroscopy with the Monte Carlo method

Bosbach, Konstantin E.[1]*, Stagg, Charlotte J.[2], Clarke, William T.[2]

[1]*Affiliation: University Medical Center, Albert-Ludwigs-Universität, Freiburg, Germany*

[2]*Affiliation: Wellcome Centre for Integrative Neuroimaging, University of Oxford, UK*

* corresponding author, konstantin.bosbach@mars.uni-freiburg.de

Magnetic Resonance Spectroscopy (MRS) measures non-invasively concentrations of neurochemicals in the living human brain. Signal-to-noise (SNR) of MRS is about five to ten thousand times lower than Magnetic Resonance Imaging (MRI) brain imaging. Detectability of the primary inhibitory neurotransmitter γ-aminobutyric acid (GABA) with non-edited single-voxel MRS is marginal with clinically-available MRI hardware. Here Monte Carlo simulations are used to explore our ability to detect changes in low concentration neurochemicals using clinical 3 tesla (3T) MRI, and using ultra-high field 7T MRI. Tools developed will enable researchers to effectively plan and power neuroscience and clinical MRS research studies quickly.

Introduction GABA is the main inhibitory neurotransmitter in the human central nervous system. Previous research has shown its importance both in understanding key brain processes, like plasticity [1], aging and development [2], as well as understanding disease pathophysiology and treatment, e.g. in depression [3].

In vivo neurotransmitter concentrations, including GABA, can be measured using MRS techniques, applied using MRI scanner hardware. MRS quantitatively detects protons (1H atoms) within the subject's brain, estimating their distribution in different molecules by the unique fingerprint (chemical shifts [4]) of each individual neurochemical [5]. However, due to low SNR, long acquisitions are needed to achieve sufficient SNR to measure concentrations accurately, or measurements must be averaged across groups of subjects. This effect is mitigated by moving to higher (but less common and clinically-available) field strengths of scanners (7T), which generate higher intrinsic signal. It might therefore be possible to measure low-concentration (1-3 mM) neurochamicals such as GABA using 7T MRS.

In this work we used existing 7T data to generate population averages of neurochemical MRS data and establish a forward model to generate arbitrary realistic simulated MRS data. Software is then designed to automatically assess the statistical detectability of a certain concentration change in neurochemicals (given a data quality [noise level] and number of subjects). The implementation generated will extend the open-source FSL-MRS [6] MRS toolbox software library, to allow more precise planning of trials and research by the MRS and neuroscience research community.

Method and materials To apply the Monte Carlo method, a basis concentration set is defined. By using the FSL-MRS toolbox, MRS spectra can be synthesised, as well as fitted, upon known basis metabolite spectra. This forward fitting is performed through linear combination of the metabolite spectra, while optimising with Bayesian statistics. By altering the input concentrations with white noise of definable variance, a new synthetic spectrum is being generated every iteration. After fitting this spectrum, concentrations of this simulated measurement are returned.

In this example, in vivo metabolite concentrations from a pre-existing dataset (19 subjects, 7T) [7] are being used, as well as three different noise strengths. The number of runs per data point is increased by a factor of two. Depicted in Figure 1, convergence can be seen in all three cases, with the biggest noise converging to well below 7% deviance from the input value. The code detects convergence by comparing mean and standard deviation, on the basis of user defined thresholds. This illustration uses the same maximum number of runs for all cases, to depict convergence speed.

Results and discussion Hitherto existing results imply the successful application of this concept like in comparable projects before. However, this method can only rectify studies at the measurability threshold, not enhance the measurement itself.

Errors might arise both from the chosen model, as well as the used model data. Extensive in vivo studies might help to recreate reality, however synthetic variations of in vivo data satisfy due to convenience.

Further enhancement of the implemented routine, as well as further tool functions, are intended.

Conclusions and future work Monte Carlo Simulations can be a reliable way to approximate the feasibility of measurements, given their precision and resource requirements, substantially expanding the possibilities of this technique.

When fully developed, this routine may complement the existing open-source fitting software library FSL-MRS, providing a practical tool for researchers and clinicians to plan their studies measurements.

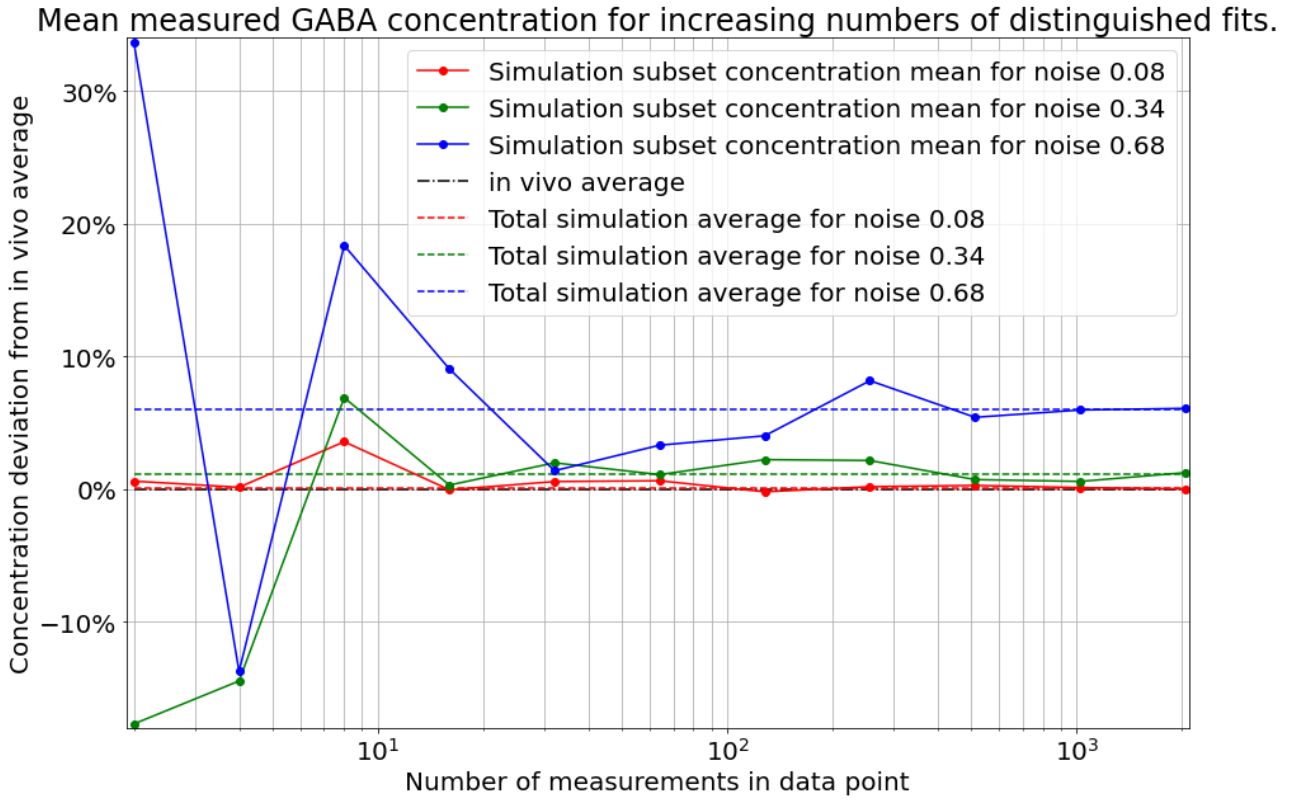

Figure 1: Monte Carlo Simulated noise resilience of the GABA MRS measurement. Three simulations of different noise. Number of runs is increased by factor two each step. Derivation of measurement relative to input concentration, in all cases well below 7%.

Bibliography

[1] VM. Karlaftis et al., “Brain stimulation boosts perceptual learning by altering sensory GABAergic plasticity and functional connectivity”, bioRxiv, 2021.

[2] J. Kolasinski et al., “The dynamics of cortical GABA in human motor learning”, J Physiol, vol. 597, pp. 271-282.

[3] RS. Duman, G. Sanacora, and JH. Krystal, “Altered Connectivity in Depression: GABA and Glutamate Neurotransmitter Deficits and Reversal by Novel Treatments.” Neuron, vol. 102(1):, pp. 75-90, 2019.

[4] J. Yao, HJ. Dyson, and PE. Wright. “Chemical shift dispersion and secondary structure prediction in unfolded and partly folded proteins”, FEBS Letters, vol. 419, 1997.

[5] Robin A. de Graaf, In vivo NMR spectroscopy : principles and techniques, 3rd ed, John Wiley & Sons Ltd., 2019.

[6] [19 subjects, Siemens Magnetom 7T, 32 channel head coil “1Tx32Rx”], kindly provided by Dr Barron and Ms Koolschijn (WIN, University of Oxford).

[7] W.T. Clarke, C.J. Stagg, and S. Jbabdi, "FSL-MRS: An end-to-end spectroscopy analysis package", Magnetic Resonance in Medicine, vol. 85, issue 6, pp. 2950-2964, June 2021.

Ethics approval

This research does not require ethics approval.

Conflict of interest

The authors declare no conflict of interest in relation to this work.

Funding Resources

KEB ist funded by a Scholarship of the Konrad Adenauer Foundation.

CJS and WTC are funded by a Sir Henry Dale Fellowship, CJS is also funded by the Wellcome Trust and the Royal Society.

2022 Proceedings of the 4th International Conference on Trauma Surgery Technology
Editors: WA Bosbach, JF Senge, P Dlotko

Session 3 – Medical applications

VBA simulations of hospital operations – case study on Covid-19 vaccine rollout schemes under resource scarcity

Wolfram A. Bosbach[1,2]*, Martin Heinrich[1,2,3], Rainer Kolisch[4], Christian Heiss[1,2]

[1] Department of Mathematics and Statistics, University of Reading, Whiteknights, Reading, United Kingdom, RG6 6AX.

[2] Institute of Cardiovascular and Metabolic Research, University of Reading, Whiteknights, Reading, United Kingdom, RG6 6AA.

[1] Experimental Trauma Surgery, Justus Liebig University of Giessen, Giessen, Germany

[2] Department of Trauma, Hand, and Reconstructive Surgery, University Hospital of Giessen, Giessen, Germany

[3] Covid-19 Emergency Taskforce, University Hospital of Giessen, Giessen, Germany

[4] TUM School of Management, Technical University of Munich, Munich, Germany

* corresponding author, wbosbach@mytum.de

During the worldwide Covid-19 pandemic, hospitals had to prioritize staff for the initial rollout of vaccines after those became available in late 2020. In spite of guidelines from state agencies, confusion existed about what an optimal rollout plan is in this situation. An open access simulation model was implemented in VBA and run under parameter variation. A rollout scheme assigning vaccine doses to hospital staff primarily by staff's pathogen exposure maximizes the predicted open hospital. In particular nursing staff benefits from an exposure focused rollout.

Introduction During the worldwide Covid-19 pandemic, SARS-CoV-2 vaccines became available in North America in late 2020 and in Europe in early 2021. Due to the scarcity and state rationing of these vaccine doses, hospitals had to prioritize staff in the initial vaccine rollout. In spite of the availability of guidelines from state agencies, confusion existed about what an optimal rollout plan is [1,2]. The weighing in of factors such as hierarchical importance [3,4], or student status [5] can alter the prioritisation plan. The model results were made available as preprint[6] and published[7].

Methods A model hospital was simulated in Visual Basic for Application (VBA) and its open capacity calculated. The study assumed that the maximisation of open hospital capacity maximises patient benefit. Staff are vaccinated in the VBA model by two different rollout schemes which can then be compared to each other. In a purely **hierarchical order top down** prioritisation argumentation is that higher ranking staff are fewer in number, more important as individuals for the functioning of the hospital, and that they are of greater age which can increase the transmission probability of the pathogen [3,4]. The alternative

rollout scheme primarily based on **exposure to the pathogen**. The code and its embedded version in Microsoft-Excel are available open access under the GNU General Public License version 3, or any later version (doi.org/10.5281/zenodo.4589333)[8].

Results and Conclusions The model demonstrates that the rollout scheme assigning vaccine doses to staff primarily by staff's pathogen exposure maximizes the predicted open hospital capacity. The rollout based on a purely hierarchical prioritization leads to reduced predicted open hospital capacity. Resource scarcity and greater disease activity increase the observable difference. Social effects need to be considered; in particular nursing staff benefits from the exposure focused scheme.

The study is calculated for parameters of SARS-CoV-2. The methodology is equally applicable to other infectious diseases. Mostly gone unnoticed in Europe and North America, the list of major infectious disease outbreaks during the 25 years before the SARS-CoV-2 pandemic included in for example Hong Kong avian flu H5N1 in 1997, SARS in 2003, swine flu 2009, and avian flu H7N9 in 2013 [9]. In the future, a vaccine prioritisation in the general population and amongst hospital staff against another infectious disease under vaccine shortage might be needed again.

Bibliography

(1) Overview of the implementation of COVID-19 vaccination strategies and vaccine deployment plans in the EU/EEA https://www.ecdc.europa.eu/sites/default/files/documents/Overview-of-COVID-19-vaccination-strategies-deployment-plans-in-the-EU-EEA.pdf (accessed Feb 26, 2021).

(2) CDC's Covid-19 vaccine rollout recommendations https://www.cdc.gov/coronavirus/2019-ncov/vaccines/recommendations.html (accessed Feb 23, 2021).

(3) Guo, E.; Hao, K. This is the Stanford vaccine algorithm that left out frontline doctors https://www.technologyreview.com/2020/12/21/1015303/stanford-vaccine-algorithm/ (accessed Feb 23, 2021).

(4) Bernstein, L.; Beachum, L.; Knowles, H. Stanford Apologizes for Coronavirus Vaccine Plan That Left out Many Front-Line Doctors. The Washington Post. Washington, DC, USA December 19, 2020.

(5) Nabavi, N. Covid-19 Vaccination for Medical Students: The Grey Area. BMJ Student 2021, 372 (n261). https://doi.org/10.1136/bmj.n261

(6) Bosbach, W. A.; Heinrich, M.; Kolisch, R.; Heiss, C. Maximisation of Open Hospital Capacity under Shortage of SARS-CoV-2 Vaccines. medRxiv 2021, 03 (08), 21253150. https://doi.org/10.1101/2021.03.08.21253150

(7) Bosbach, W. A.; Heinrich, M.; Kolisch, R.; Heiss, C. Maximization of Open Hospital Capacity under Shortage of SARS-CoV-2 Vaccines-An Open Access, Stochastic Simulation Tool. Vaccines 2021, 9 (6), 546. https://doi.org/10.3390/vaccines9060546

(8) Bosbach, W. A. Open-Access Supplement: Maximisation of Open Hospital Capacity under Shortage of SARS-CoV-2 Vaccines. zenodo 2021. https://doi.org/10.5281/zenodo.4589333

(9) Ching, F. Bird Flu, SARS and Beyond. In 130 Years of Medicine in Hong Kong; Hong Kong, PRC, 2018; pp 381–434. https://doi.org/10.1007/978-981-10-6316-9_14

Ethics approval

Research does not require ethics approval.

Conflict of interest

The authors declare that there are no conflicting interests.

Funding sources

The Deutsche Forschungsgemeinschaft (DFG) provided mobility funds through grant BO 4961/6-1.

2022 Proceedings of the 4th International Conference on Trauma Surgery Technology
Editors: WA Bosbach, JF Senge, P Dlotko

Automated Evaluation of the Whole Body's Muscle-fat Composition by Machine Learning for Magnetic Resonance Images (MRI)

Ramedani, Saied[1,2,3*], Von Tengg-Kobligk, Hendrik[2], Morhard, Christoph[3], Daneshvar Ghorbani, Keivan[2]

[1] Graduate School of Cellular and Biomedical Sciences, University of Bern, Bern, Switzerland

[2] Department of Diagnostic, Interventional and Pediatric Radiology, Bern University Hospital, University of Bern, Bern, Switzerland

[3] ProKanDo GmbH, Elfriede-Breitenbach-Str. 38a, 71640, Ludwigsburg, Germany

* corresponding author, saied.ramedani@prokando.de

This study is establishing a new Machine learning technique for whole body segmentation that is also feasible with a limited amount of data.

Introduction MRI as an imaging method can assess the volume of body components. The latest developments in MRI technology (e.g., the Dixon sequence) have further improved soft tissue contrast and measurement accuracy of fat infiltration in skeletal muscle [1].

Manual segmentation is tedious, time-consuming, and inconvenient for large-scale studies. Therefore, numerous studies have been done to provide automatic segmentation methods for MRI images recently. But despite the significant advances in methods that have been presented in the literature, no explicit automatic whole-body MRI segmentation framework is available which uses all four sequences of the Dixon technique in order to accurately segment fat and muscle, while also segmenting muscle types.

The aim of this study is to develop a novel machine learning based and fully automated muscle-fat body composition assessment framework that completely leverages the combination of all four sequences generated by the Dixon technique.

Method and materials The key principle of our proposed approach is to utilize the image information provided by the four contrast images of the Dixon MRI. The approach can be summarized into three major modules:

(1) Pre-processing module

(2) The ML model, is learned from the training set and then used for classification of the target images

(3) Post-processing module. The performance of a segmentation model is usually evaluated by a set of metrics, which are generally used for semantic segmentation models.

To evaluate the performance of our proposed CNN model, we use two different test datasets and compare the results of our model on these datasets with some reference segmentation methods that are considered as state-of-the-art in biomedical image segmentation.

Results and discussion In the first attempt to train the model, we manually segmented the lower limb region with 6 labels and trained it using them. Even with a training dataset of only 14 patients (whole-body MRI), the

proposed method achieved an average mean dice coefficient of 0.86 across all classes.

The proposed model is modular and non-specific and can therefore be easily adapted to classification tasks in other domains. To demonstrate its applicability in image segmentation, we have used our model on the BraTS Dataset [2–4]. Due to hardware limitations, we only used 10% of all training data as a training set, which includes 28 patinets. The results place us among the top ranked teams in the BraTS 2018 Challenge!

Conclusions and future work Although this work is still in progress, it already demonstrates the great potential that a system capable of performing high-quality, automated whole-body MRI segmentations could bring to a variety of medical imaging applications (e.g., brain tumor segmentation). Furthermore, this study showed that the problem of limited data can be overcome with our novel model.

Next, we will further develop the model so that it can segment all major muscle groups and their fat content.

Bibliography

[1] J. Ma, “Dixon techniques for water and fat imaging,” Journal of magnetic resonance imaging : JMRI, vol. 28, no. 3, pp. 543–558, 2008, doi: 10.1002/jmri.21492.

[2] B. H. Menze et al., “The Multimodal Brain Tumor Image Segmentation Benchmark (BRATS),” IEEE transactions on medical imaging, vol. 34, no. 10, pp. 1993–2024, 2015, doi: 10.1109/TMI.2014.2377694

[3] S. Bakas et al., “Advancing The Cancer Genome Atlas glioma MRI collections with expert segmentation labels and radiomic features,” Scientific data, vol. 4, p. 170117, 2017, doi: 10.1038/sdata.2017.117.

[4] S. Bakas et al., “Identifying the Best Machine Learning Algorithms for Brain Tumor Segmentation, Progression Assessment, and Overall Survival Prediction in the BRATS Challenge,” Nov. 2018. [Online]. Available: http://arxiv.org/pdf/1811.02629v3

Ethics approval

Ethics approval obtained from Ethics Commission of the Canton of Bern under number 2021-00846.

Conflict of interest

The authors declare that there are no conflicts of interest.

Funding sources

This study was financially supported by ProKanDo GmbH under a cooperation agreement with the University of Bern.

2022 Proceedings of the 4th International Conference on Trauma Surgery Technology
Editors: WA Bosbach, JF Senge, P Dlotko

Towards automatic comparison between planned stereotactic radiosurgery dose distributions and those measured from high-definition 3D gel dosimetry images

Maryański Marek[1]*, Marszewska Marta[1], Winiecki Janusz[2]

[1] *Institute of Nanotechnology and Material Science, Gdańsk University of Technology; Gdańsk, Poland*

[2] *Medical Physics Department, prof. Franciszek Lukaszczyk Memorial Oncology Center, Bydgoszcz, Poland*

* corresponding author, marek.maryanski@pg.edu.pl

We aim to improve metrics for automatically comparing planned vs. measured 3D dose distributions in stereotactic radiosurgery.

Introduction In stereotactic radiosurgery and radiotherapy, complex dose distributions with steep gradients are delivered at elevated dose levels. It is critical that both dosimetric and geometric accuracy of treatments are routinely assessed. Patient-specific quality assurance (PSQA) typically uses tissue-equivalent phantoms containing multiple radiation detectors for measuring 3D dose distributions actually delivered. The most complete data are obtained with gel dosimeters that change local optical density in proportion to absorbed radiation dose. Optical tomography of exposed gel phantoms can generate 3D maps of dose distributions with 1 mm spatial resolution and dosimetric uncertainty smaller than 2%. However, proper metrics and software are needed to deliver useful results quickly enough.

Method and materials A commonly used gamma evaluation tool generates a scalar field that is a function of planned and measured doses and preselected tolerances for distance-to-agreement (DTA) and dose-difference (DD) [1]. Gamma above 1 anywhere indicates unacceptable deviation from the plan at that point. Gamma may be interpreted as the closest geometric distance between the two distributions in a 4-dimensional Euclidean space (dose + distance). Computationally, it requires either a costly interpolation of sparse 3D data or a subdivision of a measured isodose surface into simplexes and then computing the closest distance between any planned point and these simplexes using matrix multiplication and inversion. A pass/fail score is determined according to appropriate quality assurance criteria. Exhaustive searches are required in this method, and the interpretation is not intuitive enough for the radiation oncologist. Also, gamma results are not always in agreement with dose-volume histograms (DVH) that are a gold standard for radiation oncology treatment plan evaluation.

In the method developed here, a gamma-equivalent “sigma” is calculated instead using local dose gradients, hence its computation time is significantly shorter than any of gamma-computing algorithms [2]. Sigma also has an intuitively simple statistical interpretation as the ratio of the local dose

difference to a user-accepted standard deviation of the local dose. Also, DTA tolerance may be preselected in sigma at zero when needed (e.g. in DVH analysis), which is not possible in gamma.

In addition, centers of mass of 3D dose clouds are computed for both planned and measured dose distributions, then a translation vector is determined that aligns the clouds better and minimizes sigma.

Results and discussion The method described here has been successfully applied to CyberKnife radiosurgery and radiotherapy and to proton therapy [2]. Software implementation still needs streamlining to save user time.

Conclusions and future work Since the introduction of gamma evaluation tool, many efforts have been made to improve it. The new solution presented here has been positively validated. Two additional steps are being contemplated. Axes of ellipsoids of inertia of dose clouds treated as rigid bodies will be determined and corrective rotational shifts will be applied in order to minimize sigma still further. Second, topology of remaining differences, if significant, will be analyzed in order to identify their likely sources.

Bibliography

[1] Low DA, Dempsey JF. Evaluation of the gamma dose distribution comparison method. Med Phys. 2003;30(9):2455-2464. doi:10.1118/1.1598711

[2] M. Maryanski, High-Definition 3D Dosimetry for End-To-End PatientSpecific Treatment Delivery Verification, Chapter #10, in Maria F. Chan (Ed.), Recent Advancements and Applications in Dosimetry, Nova Science Publishers, 2018. ISBN 978-1-53613-759-0

Conflict of interest

The authors declare that there are no conflicts of interest.

Funding sources

The study is being supported in part by a grant from the Polish government's NAWA "Polish Returns" Program and by an IDUB/RADON grant.

2022 Proceedings of the 4th International Conference on Trauma Surgery Technology
Editors: WA Bosbach, JF Senge, P Dlotko

Magnet resonance imaging of congenital vascular malformations

F. Haupt[1], A. Huber[1], C. Calastra[1], A. Tuleja[2], J. Rössler[3], I. Baumgartner[2] and H. von Tengg-Kobligk[1]

[1] Inselspital Bern, Department of Diagnostic, Interventional and Pediatric Radiology, Inselspital, Bern University Hospital, University of Bern, Bern, Switzerland, Bern, Switzerland

[2] Inselspital Bern, Division of Angiology, Swiss Cardiovascular Center, Inselspital, Bern University Hospital, University of Bern, Switzerland, Bern, Switzerland

[3] Inselspital Bern, Pediatric Hematology/Oncology, Department of Pediatrics, Inselspital, Bern University Hospital, University of Bern, Switzerland, Bern, Switzerland

* corresponding author, fabian.haupt@insel.ch

Educational presentation of state of the art imaging of congenital vascular malformations.

Background Congenital vascular malformations (CVM) are defects of the vascular system, which develop during angiogenesis in utero. CVMs are divided in high flow and low flow malformations and are classified according to the diseased vessel type. Magnetic resonance imaging (MRI) is the current state oft he art method for the morphological characterization of CVMs, regarding extent, involved compartments and lesion composition.

The utilization of morphological T1w and T2w sequences allows tissue characterization of suspected vascular malformations, i.e. to differentiate between hemovascular and lymphatic components. MR angiography (MRA) with Gadolinium-based contrast agents allows the visualization and assessment of the perfused vascular portion of malformations. The continuous acquisition using time resolved MRA allows semiquantitative analysis of the hemodynamics in vascular malformations.

Methods CVM imaging requires multiplanary T2w sequences with fat saturation. T1w sequences prior and post contrast agent administration are important for the visualization of the vascular portion. Time resolved MR angiography allows the characterization of CVM hemodynamics. The combination of these sequences allows to determine the extent, involved tissues/compartments and type of malformation and the identification of relevant features (i.e. thrombosis, phleboliths, bleeding). The combination of clinical and MRI findings can further help to identify syndromes like Parkes-Weber or Klippel-Trenaunay.

Conclusion MRI is the most important modality for diagnosis and therapy monitoring of CVM. The correct classification and the detection of post therapeutic changes is crucial for the stratification of the best therapy option.

Ethics approval

Ethics approval obtained from Ethics Commission of the Canton of Bern

Conflict of interest

The authors declare that there are no conflicts of interest.

Funding sources

This study was financially supported by the Swiss National Science Foundation (SNF).

2022 Group photo during session 3 – 23 April 2022

2020 Group photo – 17 Oct 2020

2019 Group photo – 12 Oct 2019

2018 Group photo – 17 Nov 2018

List of 2022 Participants

United Kingdom

Dr Burfitt, Matthew, University Aberdeen

Prof Tindall, Marcus J, University of Reading

Poland

Dr Dlotko, Pawel, Dioscuri Centre for Topological Data Analysis, Warsaw

Gurnari, Davide, Dioscuri Centre for Topological Data Analysis, Warsaw

Hellmer, Niklas, Dioscuri Centre for Topological Data Analysis, Warsaw

Marszewska Marta, Gdansk University of Technology

Prof Maryanski, Marek, Gdansk University of Technology

Switzerland

Dr Daneshvar Ghorbani, Keivan, University of Bern

Dr Haupt, Fabian, University of Bern

Ramedani, Saied, University of Bern

Germany

Bosbach, Konstantin E, Albert-Ludwigs-University, Freiburg

Dr Bosbach, Wolfram A, Justus-Liebig University of Giessen

Senge, Jan, University of Bremen

Giessen University Medical Faculty

29, Klinikstrasse

Giessen 35390

Germany

Image source: by friendly permission of Landesbetrieb Bau und Immobilien Hessen, Mr Hoffmann on 27 Sept 2018 by email.